

Aromaticity on the fly: cyclic transition state stabilization at finite temperature

Supporting Information

Tamás Rozgonyi¹, Albert Bartók-Pártay², András Stirling^{1*}

¹*Chemical Research Center of the Hungarian Academy of Sciences, Budapest, Hungary and*

²*University of Cambridge, United Kingdom*

(Dated: October 20, 2009)

I. COMPARISON OF THEORY AND EXPERIMENT

Table 1 shows the calculated activation energies (Gaussian 03¹ using the BLYP² and the B3LYP³ functionals) and the corresponding experimental values.

Table 1

molecule	BLYP	B3LYP	exp.
barbaralane	3.4	6.8	7.58 ± 0.09^a
bullvalene	8.7	12.6	13.8 ± 0.2^b

^aRef. 4; ^bRef. 5.

II. TDDFT CALCULATIONS

The TDDFT calculations have been performed within the UBLYP/aug-cc-pVTZ and UB3LYP/aug-cc-pVTZ framework³ on the TS configuration obtained from BLYP/6-31+G* calculation. For barbaralane the first excited state is triplet (³B₂), with 2.40 eV excitation energy whereas the first singlet state (¹B₂) is 4.49 eV higher in energy than the ground state. For bullvalene the first excited state (³B₁) is 2.20 eV higher than the ground state, whereas the first singlet excitation (¹B₁) requires 3.90 eV.

Comparison of the TDDFT results obtained with the BLYP and the B3LYP functionals using the aug-cc-pVTZ basis on the TS configuration shows that all the excited singlet states are underestimated by the BLYP functional relative to the B3LYP levels by 9-15 kcal/mol. This implies that as long as we remain on the singlet BLYP energy

surface we can indeed identify the reaction mechanism of the intramolecular Cope rearrangement. Therefore the BLYP functional is suitable for the present study despite its well-known tendency to stabilize delocalized structures.

III. IRC CALCULATIONS: DETERMINATION OF THE CUTOFF DISTANCE

In Ref. 6 it has been shown that the inflection point of the IRC curve can be very efficiently used to interpret the corresponding chemical reactions. The reaction can be divided into two phases: a phase dominated by structural changes (preparation phase) and a phase dominated by electronic effects (transition region). The two zones can be separated by locating the inflection point of the IRC curve, where the so called reaction force: $-\frac{\partial V(s)}{\partial s}$ is maximal (s is the intrinsic reaction coordinate, $V(s)$ is the potential energy as a function of s). In this study we also used this idea to separate the atomic configurations into two classes: reactant (\mathcal{R}) and transition (\mathcal{T}) states. In Figs. 1 and 2 we show the intrinsic reaction coordinate (IRC) paths of the rearrangements along with their derivatives with respect to the IRC. For barbaralane the minimum of the derivative curve (ie. the point of inflection of the IRC curve) is at 2.03 bohr $\text{amu}^{-1/2}$ which gives 1.75 Å for the forming CC distance. For bullvalene the minimum point is at 2.34 bohr $\text{amu}^{-1/2}$ corresponding to 1.73 Å CC distance.

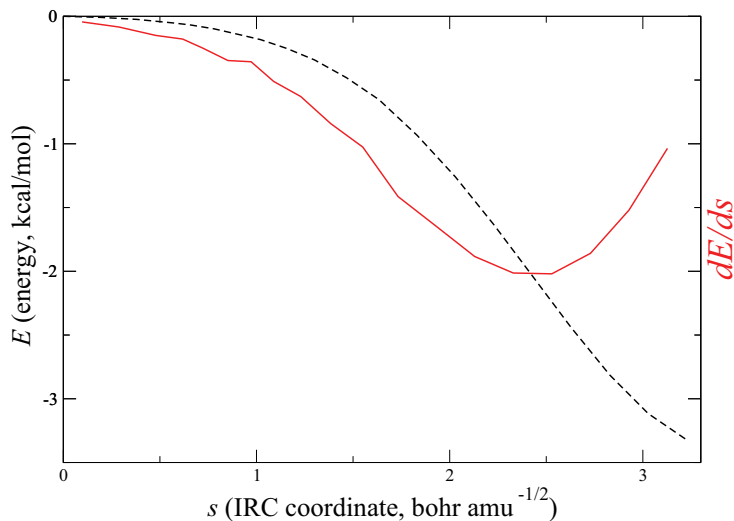


FIG. 1: IRC curve and its derivative for barbaralane

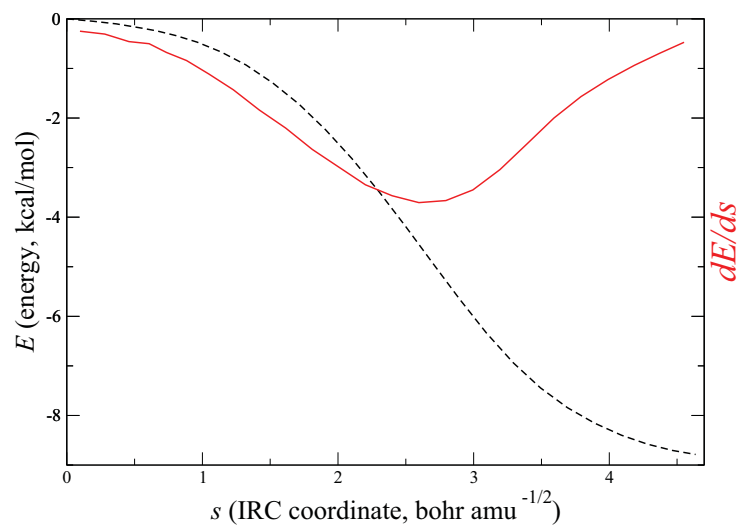


FIG. 2: IRC curve and its derivative for bullvalene

IV. NICS AT 0 K

In Fig. 3 we have labelled the carbon atoms of the barbaralane molecule which participate in the intramolecular rearrangement. We have considered these atoms to construct their least-square plane which has been used to define the point for calculating the NICS value. For bullvalene we constructed the planes similarly but in each single reaction we had to identify the 6 carbon atoms participating in the rearrangement.

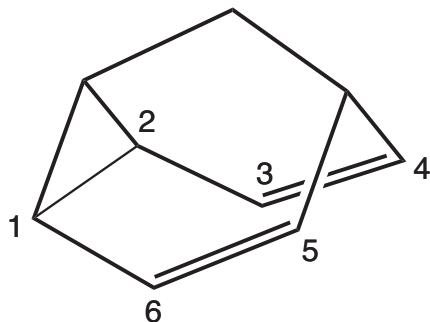


FIG. 3: The 6 carbon atoms in barbaralane defining the plane for the NICS calculations.

Figs. 4 and 5 show the evolution of a set of NICS values of barbaralane and bullvalene calculated along their IRC paths. For defining this set of points we have calculated the center of mass point (M) of the 6 C atoms participating in the rearrangements and determined their least-square plane (LSP). The points lie on a line passing through M and perpendicular to the LSP at regular intervals of 0.25 \AA starting at 1.5 \AA from M in the direction outward from the molecule. We see that the NICS value at 0.5 \AA distance from M shows the largest variation going from the TS to the reactant state for both molecules. Therefore the variation of aromaticity along the trajectories has been followed by the NICS calculated at this point.

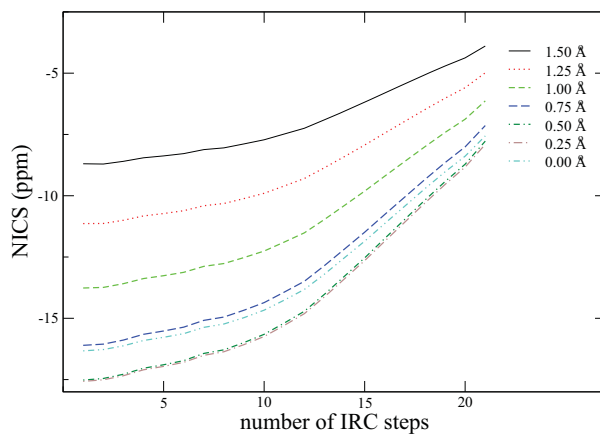


FIG. 4: Variation of the NICS values of barbaralane calculated at several distances from the center of the reacting 6 carbon atoms along the IRC path.

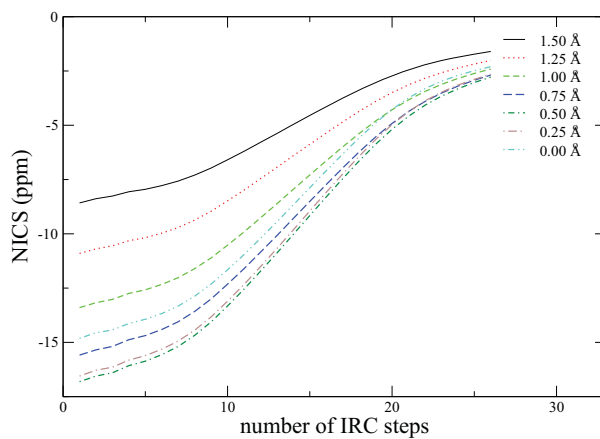


FIG. 5: Variation of the NICS values of bullvalene calculated at several distances from the center of the reacting 6 carbon atoms along the IRC path.

V. EVOLUTION OF THE CC BONDS

To demonstrate that the intramolecular Cope reactions are not accompanied by any side reactions during the simulations we present a figure where the evolution of all the CC bonds of **1** at 1000 K are displayed. The blue and red curves correspond to the reacting CC bonds, the other curves belong to the remaining CC bonds. Clearly, these bonds do not break during the simulation, albeit feature occasionally large fluctuations. Similar behaviour can be observed at all the selected temperatures.

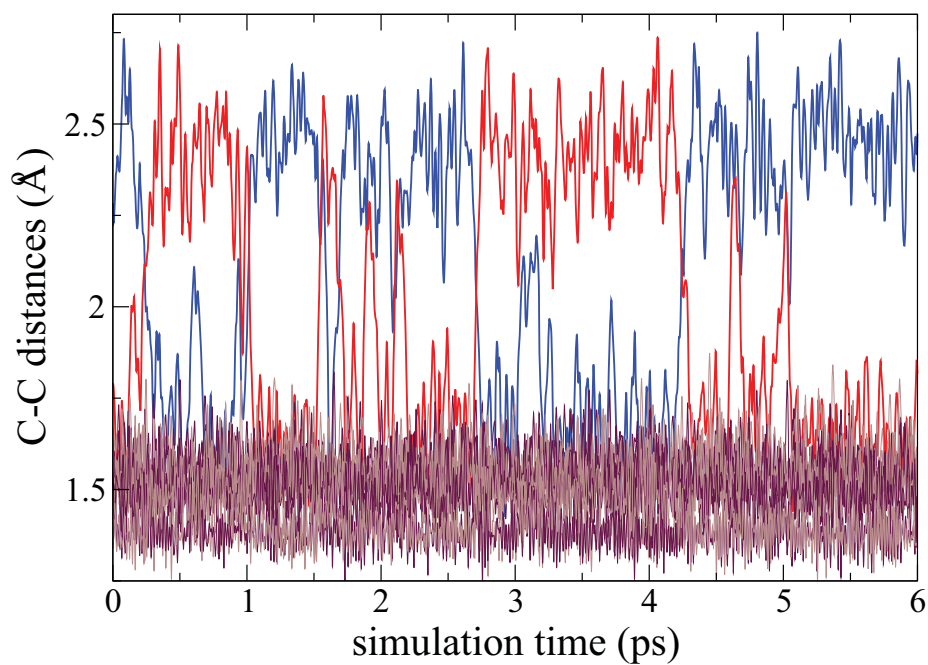


FIG. 6: Structural evolution of **1** at 1000 K during 6 ps.

VI. NICS ON THE DYNAMICAL PATHS: BULLVALENE

In the main text we have presented graphs showing the correlation between the variation of the NICS and the $|d_1 - d_2|$ values in the case of barbaralane. Fig. 7 shows that this correlation is valid also for bullvalene. In this figure we have plotted the NICS and the $|d_1 - d_2|$ quantity during three randomly chosen intervals of 160 fs of the trajectories at 5 different temperatures. In each case the two quantities feature strongly correlated behaviour.

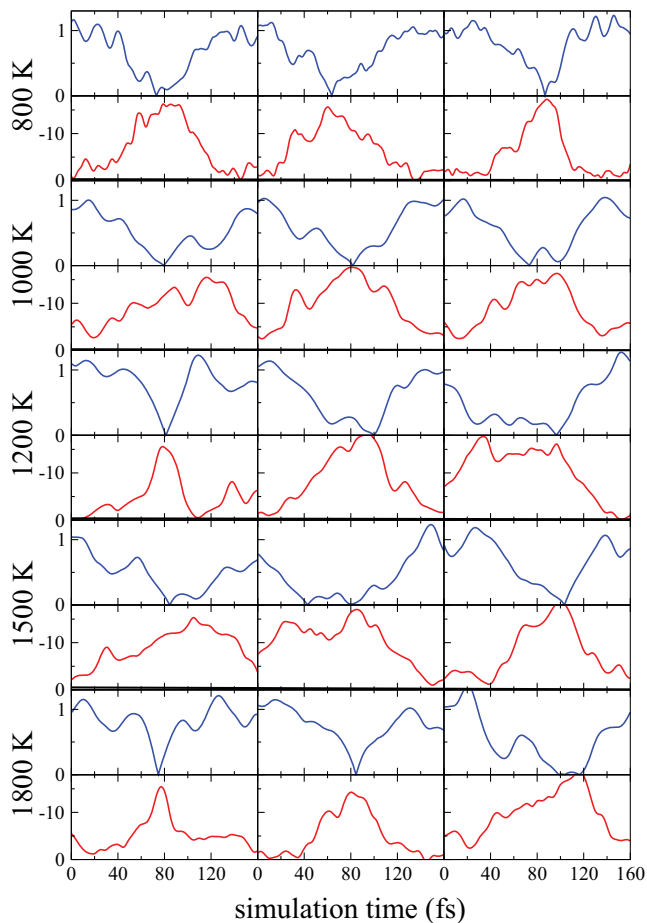


FIG. 7: Evolution of the $|d_1 - d_2|$ reaction coordinate (blue curves) and the NICS value (red curves) representative of the aromaticity of the six participating carbon atoms of **2** within a short time period of 160 fs at 3 randomly chosen times at various temperatures. The NICS axes are reversed for better visualization.

VII. FREE ENERGY CALCULATIONS: REACTION COORDINATE AND ERROR ESTIMATION

In this study the reaction coordinate s is discretized and represents two states, the reactant (\mathcal{R}) and the transition \mathcal{T} states. The activation free energy is calculated according to Eq. 1:

$$\Delta F = -k_B T \ln \left(\frac{P(\mathcal{T})}{P(\mathcal{R})} \right) \quad (1)$$

where ΔF is the activation free energy, $P(\mathcal{T})$ and $P(\mathcal{R})$ are the probability of finding the system in the transition and reactant states, respectively. The probabilities are calculated for the whole trajectories. For barbaralane we employ a simple structural criterion for classifying the configurations: if the lengths of bonds \mathbf{b}_1 and \mathbf{b}_2 are both larger than d_0 , the configuration is in \mathcal{T} , otherwise belongs to \mathcal{R} , where $d_0 = 1.75 \text{ \AA}$ (see Scheme 1 in the text for labeling). For bullvalene this criterion is not suitable as each CC bond may take part in the reaction. Therefore in the case of bullvalene we used the cumulative coordination number (CCN) as reaction coordinate. The *CCN* is the sum of the individual coordination numbers (CNs) of the carbon atoms. The CN of a given carbon atom gives the number of other carbon atoms forming bond with it. To define a C-C bond we simply used a structural criterion, similarly to the case of barbaralane: if the C-C distance is smaller than d_0 , then there is a bond between the two C atoms, otherwise not. For bullvalene $d_0 = 1.73 \text{ \AA}$ (obtained from the IRC, see earlier). In this way we obtain $CCN = 24$ for state \mathcal{R} and 22 for state \mathcal{T} .

The limited statistics provided by the trajectories can be characterized by the error margins of the calculated activation free energy values using Eq. 2:

$$\sigma(\Delta F) = k_B T \sqrt{\frac{1}{N_{trans}} \left(\frac{1}{P(\mathcal{R})} + \frac{1}{P(\mathcal{T})} \right)} \quad (2)$$

where $\sigma(\Delta F)$ is the error of the estimation of ΔF and N_{trans} is the number of transitions between states \mathcal{R} and \mathcal{T} .

¹ Frisch, M. J.; Trucks, G. W.; Schlegel, H. B.; Scuseria, G. E.; Robb, M. A.; Cheeseman, J. R.; Montgomery, J. A.; Vreven, T.; Kuding, K. N.; Burant, J. C.; Millam, J. M.; Iyengar, S. S.; Tomasi, J.; Barone, V.; Mennucci, B.; Cossi, M.; Scalmani, G.; Rega, N.; Petersson,

- G. A.; Nakatsuji, H.; Hada, M.; Ehara, M.; Toyota, K.; Fukuda, R.; Hasegawa, J.; Ishida, M.; Nakajima, T.; Honda, Y.; Kitao; Nakai, H.; Klene, M.; Li, X.; Knox, J. E.; Hratchian, H. P.; Cross, J. B.; Bakken, V.; Adamo, C.; Jaramillo, J.; Gomperts, R.; Stratmann, R. E.; Yazyev, O.; Austin, A. J.; Cammi, R.; Pomelli, C.; Ochterski, J. W.; Ayala, P. Y.; Morokuma, K.; Voth, G. A.; Salvador, P.; Dannenber, J. J.; Zkrzewski, V. G.; Dappich, S.; Daniels, A. D.; Strain, M. C.; Farkas, O.; Malick, D. K.; Rabuck, A. D.; Raghavachari, K.; Foresman, J. B.; Ortiz, J. V.; Cui, Q.; Baboul, A. G.; Clifford, S.; Cioslowski, J.; Stefanov, B. B.; Liu, G.; Liashenko, A.; Piskorz, P.; Komaromi, I.; Martin, R. L.; Fox, D. J.; Keith, T.; Al-Laham, M. A.; Peng, C. Y.; Nanykkara, A.; Callacombe, M.; Gill, P. M. W.; Johnson, B.; Chen, W.; Wong, M. W.; Gonzalez, C.; Pople, J. A., *Gaussian 03*; Gaussian, Inc.: Wallingford, CT, 2004.
- ² Becke, A. *Phys. Rev. A* **1988**, *38*, 3098-3100; Lee, C.; Yang, W.; Parr, R. *Phys. Rev. B* **1988**, *37*, 785-789.
- ³ Becke, A. D. *J.Chem.Phys.* **1993**, *98*, 5648-5652. Lee, C.; Yang, W.; Parr, R. *Phys. Rev. B* **1988**, *37*, 785-789.
- ⁴ Jackman, L. M.; Fernandes, E.; Heubes, M.; Quast, H. *Eur. J. Org. Chem.* **1998**, 2209-2227.
- ⁵ Moreno, P. O.; Suarez, C.; Tafazzoli, M.; True, N. S.; LeMaster, C. B. *J. Phys. Chem.* **1992**, *96*, 10206-10212.
- ⁶ Politzer, P.; Murray, J. S.; Lane, P.; Toro-Labbé, A. *Int. J. Quant. Chem.* **2007**, *107*, 2153-2157.